PROSPECTS AND PROSPECTING ALONG THE N=Z LINE*

W. GELLETLY

Physics Department, University of Surrey
Guildford, Surrey Gu2 5XH, England

(Received November 18, 1994)

The reasons for our interest in nuclei with $N = Z$ are outlined. The methods used to study the $N \sim Z$ nuclei up to $A = 100$ and the state of our knowledge of their properties are reviewed. Future experiments, involving both existing facilities and radioactive nuclear beams, designed to improve our knowledge of nuclei near the $N = Z$ line are described. Finally the Radioactive Ion Source Test (RIST) project, designed to pave the way for a full-scale radioactive beam facility at the ISIS spallation neutron source, is described and its progress reported.

PACS numbers: 23.90.+w

1. Introduction

The reasons for our interest in the atomic nuclei with $N = Z$ are not hard to find. In terms of nuclear physics they are readily deduced from Fig. 1 which shows [1] the single particle levels as a function of deformation for $N, Z = 28 - 50$. In this figure we see the well known, spherical, magic numbers at $N, Z = 40$ and 50. At the same time pronounced energy gaps are seen at $\beta = +0.4$ for $N, Z = 38$ and $\beta = -0.35$ for $N, Z = 32, 34$. The fact that the valence neutrons and protons are filling the same orbits in these nuclei reinforces the effects of the deformed shell gaps. There is now ample evidence that states with large prolate and oblate deformation and with triaxial shapes co-exist in $N = Z$ nuclei with $A \sim 60 - 80$. Inspection of Fig. 1 also reveals energy gaps at $\beta \sim +0.6$ for $N, Z = 42$. This is presumably the origin of the superdeformed states recently reported in ^{81,83}Sr and ^{84}Zr [2]. Along the $N = Z$ line itself the results of calculations such as

* Presented at the XXIX Zakopane School of Physics, Zakopane, Poland, September 5–14, 1994.

reported in [1] would suggest a progression from spherical shape at $Z \sim 28$ through oblate/prolate co-existence to a large ($\beta = 0.4$) prolate deformation for ^{76}Sr and its neighbours and then back through the same sequence to a spherical shape at ^{100}Sn. The results of a whole series of experiments [3, 4] carried out at the Daresbury Nuclear Structure Facility prior to its closure confirm the first half of this sequence.

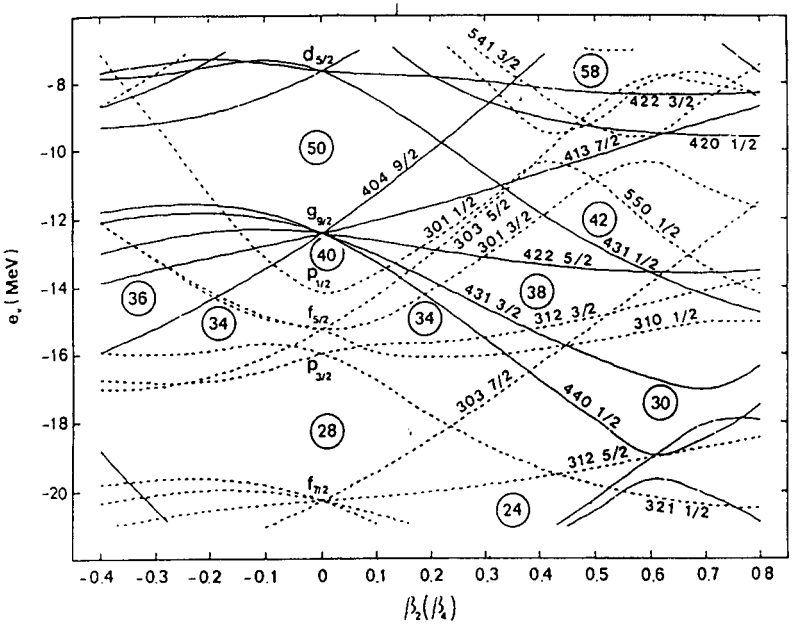

Fig. 1. The single particle levels [1] for $N, Z = 28 - 50$ as a function of deformation.

One question which immediately leaps to mind when one thinks of nuclei with $N = Z$ is what light their properties shed on isospin. In particular how does isospin mixing change with mass and angular momentum. Naively one would anticipate that isospin mixing in $N = Z$, even-even nuclei would increase with A but the relative excitation energy of the Giant Dipole Resonance will also affect it. One must have recourse to experiment to settle such questions. Only a little information [5, 6] is available on isospin as a function of angular momentum and one would dearly like more. Here one would expect states of greater isospin purity at higher angular momentum because of the lower density of states, but so far we have no evidence to test such ideas.

Our interest in these nuclei is not confined to nuclear physics. The path of the astrophysical rp-process passes [7] this way. Its exact path depends on the ground state properties of a large number of nuclei close to or on the

$N = Z$ line. The results of nuclear physics experiments are essential for our understanding of the process.

A glance at the Segré Chart shows that above ^{40}Ca the $N = Z$ line and the line of stability diverge rapidly. This has two consequences for the experiments. Firstly, the nuclei to be studied are highly neutron-deficient and secondly, the $N = Z$ line crosses the proton drip-line somewhere just above ^{100}Sn. This will eventually set some sort of limit to our studies but it also means that we may find some interesting new phenomena and expect new information on well known phenomena since the nuclei to be studied are close to the drip-line.

2. The experimental story so far

So far our knowledge and understanding of the properties of the $N \sim Z$ nuclei with $A = 80 - 100$ is derived from experiments based on studies of

(i) beta decay of nuclei produced following spallation or heavy ion fusion reactions;

(ii) heavy ion fragmentation;

(iii) prompt gamma rays emitted in heavy ion induced, fusion-evaporation reactions.

Here I will confine my remarks to *(ii)* and *(iii)* with the main emphasis being on *(iii)*. This is not to suggest that β-decay studies are not important. In nuclei with $N = Z$ they reveal much about the nature of the Weak Interaction as well as providing essential information on nuclear structure complementing studies of reaction induced gamma rays. Indeed the absence of decay studies sometimes means that we cannot readily construct level schemes from reaction studies alone.

2.1. Heavy ion fragmentation

Space is too limited here to describe the nature of heavy ion reactions [8]. Suffice to say that a large number of different reaction products are produced in such reactions. In recent years this has been exploited at MSU, GANIL, RIKEN and G.S.I., first to provide information on the properties of highly neutron-deficient and neutron-rich nuclei and secondly, to provide beams of radioactive nuclear species at high energy [8]. There are too many interesting results to detail here but the exploration [9] of the neutron halo in neutron-rich, light nuclei and the discovery of ^{100}Sn [10, 11] will suggest the flavour and interest of the overall programme.

All of these studies have much in common. Here as an exemplar I will refer the reader to the A1200 spectrometer [12] at MSU. It is shown schematically in Fig. 2. Energetic heavy ions, typically with energies 50–100 MeV/u

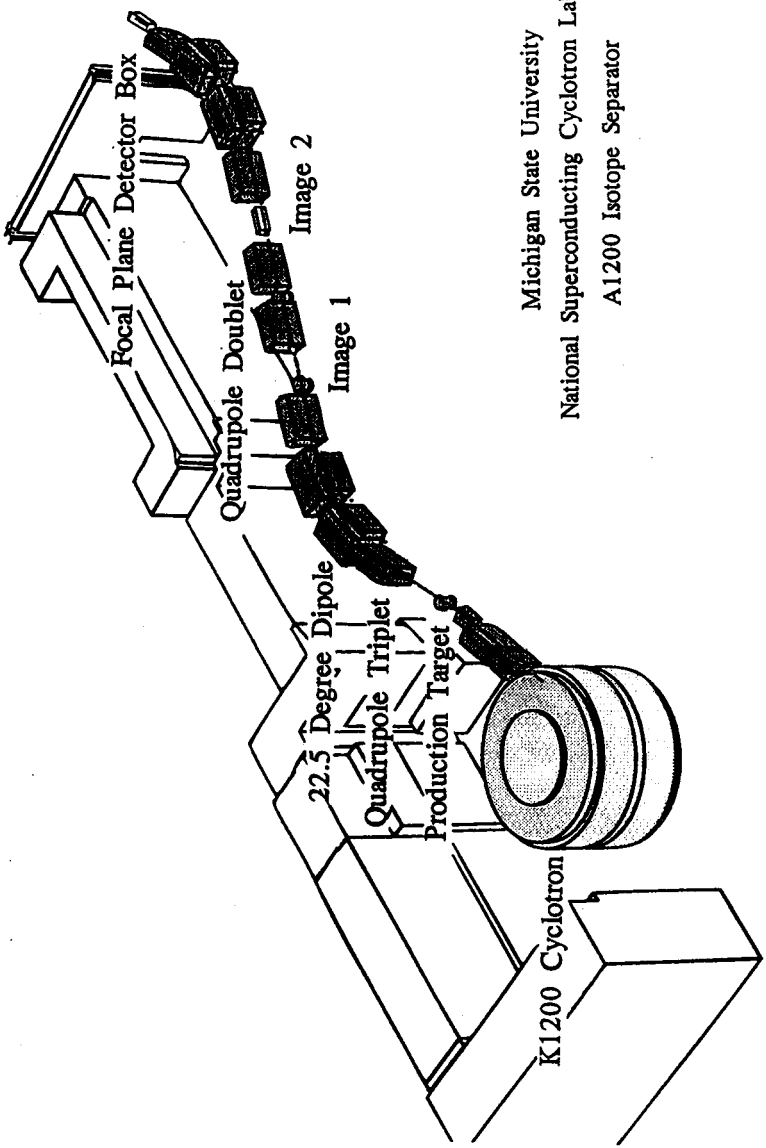

Fig. 2 A schematic diagram of the A1200 spectrometer [12] at the Michigan State University cyclotron

or greater, are focused on a thick target. Fragments produced in peripheral collisions, with a linear momentum close to that of the beam particles are focused at various points through the spectrometer. Measurements of the fields in the magnets combined with the position of an ion at the dispersive focal point marked Image 2, measured with a position-sensitive, parallel--plate avalanche counter allow the determination of magnetic rigidity $B\rho$. At the final achromatic focus a silicon detector telescope is used to give two energy loss signals and a total energy signal. These measurements, combined with the measured time-of-flight over a distance of 14 m, from Image 1 to the first element of the detector telescope, give a unique measure of Z and A for each ion.

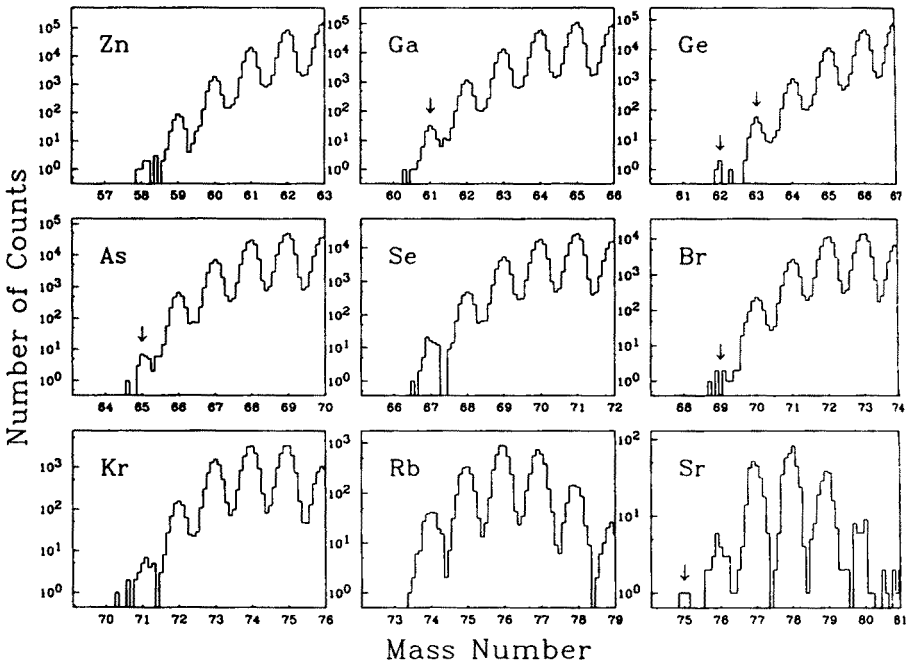

Fig. 3. Mass Spectra for $Z = 30-38$ particles recorded with the A1200 spectrometer [12]. The isotopes were produced in the bombardment of ^{58}Ni with a ^{78}Kr beam at $E/A = 65$ MeV.

Fig. 3 shows the mass spectra [13] for various elements produced in the bombardment of a 94 mg cm^{-2} thick target of ^{58}Ni with ^{78}Kr ions with $E/A = 65$ MeV. One sees clearly that isotopes with $N < Z$ are produced. Non-observation of a particular isotope implies either that it has a partial half-life less than 150 ns, the flight time through the spectrometer, or that the production cross-section is too low for it to be observed. This experiment

and the latter work of Winger *et al.* [14] shows that ^{65}As exists in its ground state with a half life of $0.19^{+0.11}_{-0.07}$ secs, and hence that it is not a termination point in the astrophysical rp-process.

2.2. Heavy ion fusion reactions

An alternative means of studying $N \sim Z$ nuclei has been to study γ-rays emitted in heavy ion induced fusion-evaporation reactions. For example at the Daresbury Nuclear Structure Facility we carried out a series of experiments involving the detection of γ-rays in an array of 20 escape-suppressed Ge detectors in coincidence with recoilling nuclei detected in an ionization chamber in the focal plane of a recoil mass separator [15]. The recoil mass separator was designed to separate the recoilling nuclei from beam particles and identify them by A and Z. In this way the γ-rays observed can be accurately assigned to a particular reaction channel.

How far have we reached in such experiments? In terms of real spectroscopy, namely producing a substantive level scheme for the product nucleus, the heaviest $N = Z$ nucleus for which we have been able to produce a level scheme with more than a few levels is ^{64}Ge [16]. As far as mirror nuclei are concerned the heaviest pair of nuclei reached so far is ^{49}Cr/^{49}Mn [5]. Beyond ^{64}Ge we were only able to see a few γ-ray transitions from the even-even, $N = Z$ nuclei [3, 4]. Brief comments on these measurements follow.

2.2.1. The ^{64}Ge nucleus

This was studied in the ^{12}C (^{54}Fe,2n)^{64}Ge reaction at 165 MeV bombarding energy. The gamma ray spectrum gated by ^{64}Ge recoils identified with the recoil mass separator is shown in the upper half of Fig. 4. In the lower half we see the resulting level scheme.

The J^{π} assignments to the negative parity band are tentative. They are based partly on systematics but the observed decays to the ground state band are clearly dipole transitions from their measured angular distributions.

In a $T_Z = 0$ nucleus such as ^{64}Ge there should be no E1 transitions between $T = 0$ states. The results imply isospin mixing and analysis [16] suggests that there is a 7% admixture of the $T = 1$ states in the $T = 0$ states in ^{64}Ge. It would clearly be interesting to study this as a function of A.

2.2.2. Mirror nuclei at high spin

The idea of the charge independence of nuclear forces is well established and isospin multiplets have been studied as a function of A. However, few measurements of isospin as a function of angular momentum have been

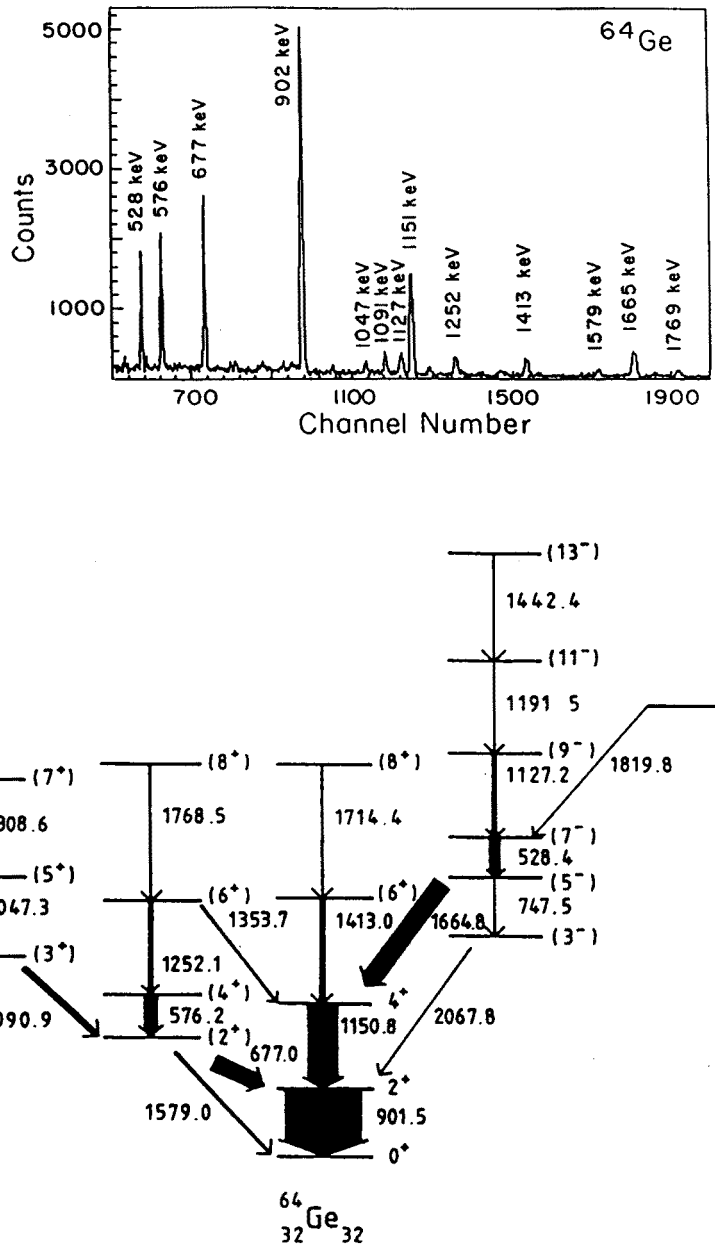

Fig. 4. Spectrum of γ-rays in coincidence with ^{64}Ge recoils produced in the ^{12}C (^{54}Fe,2n)^{64}Ge reaction. In the lower half we see the level scheme of ^{64}Ge.

made. In the bombardment of ^{12}C with ^{40}Ca we were able [5] to identify γ-rays from the mirror pair ^{49}Mn and ^{49}Cr and place them in the level

schemes shown in Fig. 5. Not surprisingly the level schemes are remarkably similar. The structures observed are also collective in character, although the number of contributing valence nucleons in the middle of the $f_{7/2}$ shell is quite small.

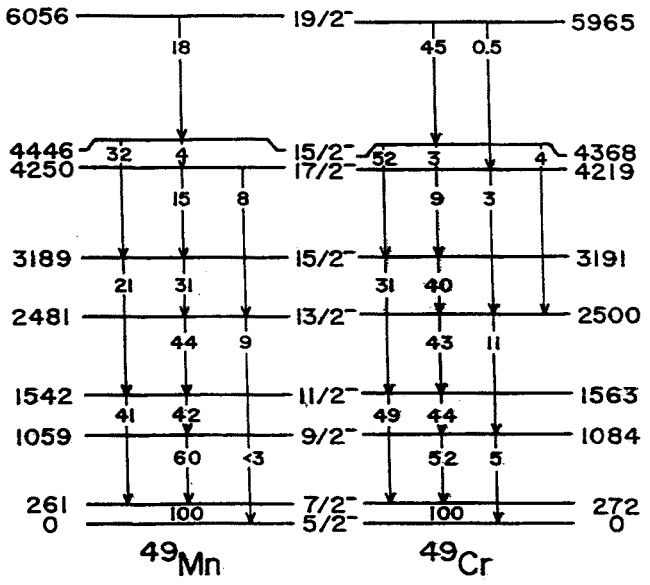

Fig. 5. A comparison of the level schemes for ^{49}Mn and ^{49}Cr.

Fig. 6 summarises one interesting aspect of the results. In this figure we see plotted $\Delta V_c = E_x(\mathrm{Mn}) - E_x(\mathrm{Cr})$, the Coulomb energy difference between the levels in the two nuclei, and the rotational frequency (ω), derived from the observed γ-ray energies, plotted as a function of angular momentum. Here it was assumed that the levels observed are collective. The Coulomb energy difference is seen to show a sudden rapid increase just at the point where we appear to get an alignment of a pair of $f_{7/2}$ protons in ^{49}Cr. This occurs at the frequency where such an alignment would be predicted by the Cranked Shell Model. In ^{49}Cr with 24 protons one would expect the protons to align first since the neutron alignment is blocked. The rearrangement of the protons will alter the Coulomb energy. In ^{49}Mn it is the neutrons which align since the protons alignment is blocked. To first order this should not affect the Coulomb energy. Thus when we examine ΔV_c we would expect an increase just at the point where the protons align.

One may see this effect as providing new information on alignments of pairs of nucleons. However, it might also be due to non-collective effects in a limited single particle space. In ^{49}Mn/^{49}Cr we would have held data for levels at higher angular momentum. It would also be interesting to look at

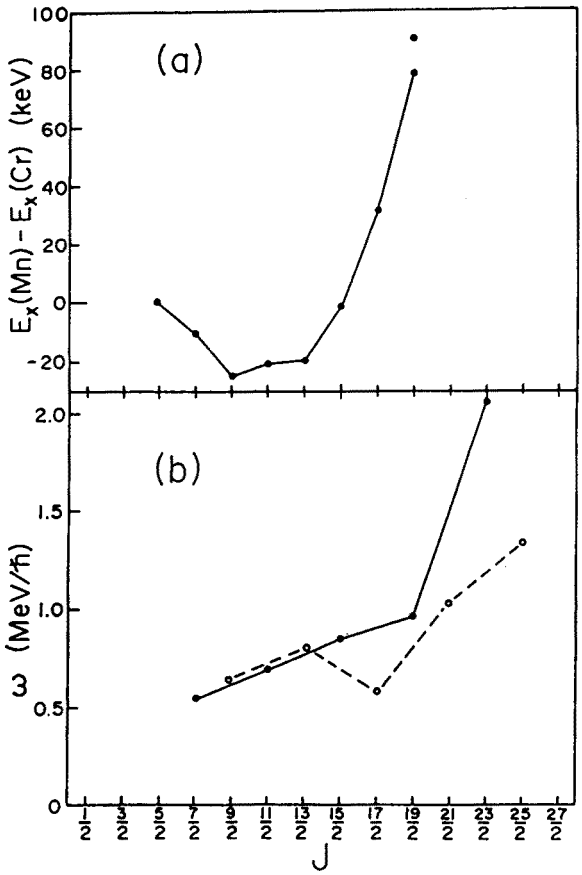

Fig. 6. Coulomb energies (upper) and rotational frequency (lower) *vs.* J for ^{49}Mn and ^{49}Cr.

the same effects in heavier nuclei where there is a larger configuration space. Just before the Daresbury accelerator was closed an attempt [17] was made to do just this by studying the ^{75}Rb/^{75}Sr mirror pair in the ^{40}Ca + ^{40}Ca reaction.

In this experiment the γ-rays were detected with the EUROGAM array. Unfortunately although EUROGAM worked well only a limited amount of recoil-γ coincidence data was obtained. This was enough to determine the ^{75}Rb level scheme shown in Fig. 7 but not to determine the corresponding level scheme for ^{75}Sr. The results suggest that a full set of data would have allowed a successful experiment.

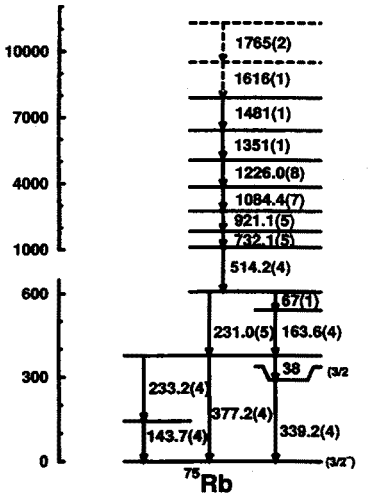

Fig. 7. Level scheme for ^{75}Rb [17].

2.2.3. The even-even, $N = Z$ nuclei

Above ^{64}Ge we were only able to observe a few γ-ray transitions in the even-even, $N = Z$ nuclei. In a series of experiments transitions were observed in all such nuclei up to ^{84}Mo [4]. In this case only a single transition was observed in the ^{28}Si (^{58}Ni, 2n)^{84}Mo reaction. In all these experiments the same strategy was pursued. The beam energy was kept close to the Coulomb barrier to limit the number of open reaction channels. The nucleus of interest also had the highest Z which could be produced, which made the Z identification from the E signal easier. Fig. 8 shows partial γ-ray spectra for ^{84}Zr, ^{84}Nb and ^{84}Mo gated by the recoilling nuclei.

TABLE I

Cross sections of the $2N$ channel used to populate $N = Z$ nuclei

Reaction	E_{LAB}(MeV)	$N = Z$ nucleus	Cross section*
^{54}Fe + ^{12}C	155	^{64}Ge	640(70)
^{58}Ni + ^{12}C	175	^{68}Se	38(16)
^{58}Ni + ^{16}O	170	^{72}Kr	60(25)
^{54}Fe + ^{24}Mg	175	^{76}Sr	10(5)
^{58}Ni + ^{24}Mg	190	^{80}Zr	10(5)
^{58}Ni + ^{28}Si	195	^{84}Mo	7(3)

* See Ref. [4] and references therein.

Table I summarises this series of measurements. The cross-section is falling with increasing Z and the limit of sensitivity with the apparatus

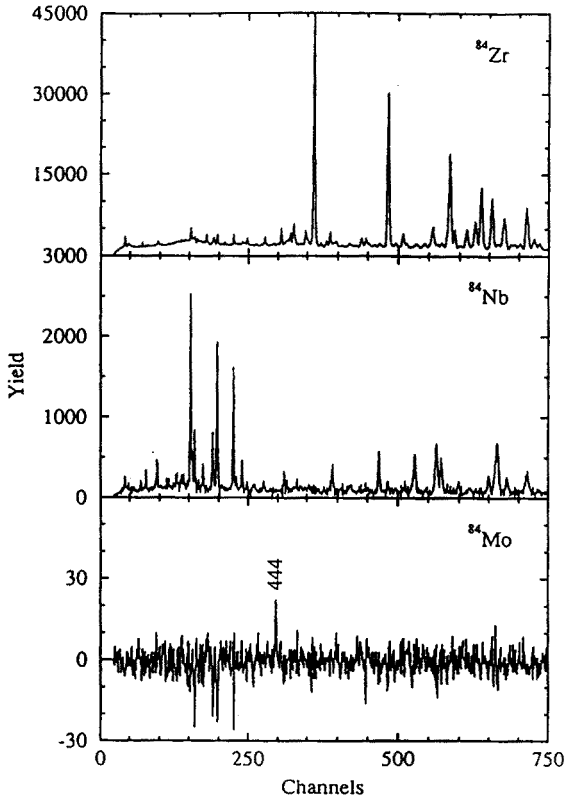

Fig. 8. Gamma ray spectra in coincidence with ^{84}Zr, ^{84}Nb and ^{84}Mo recoils produced in the bombardment of ^{28}Si with ^{58}Ni [4].

used is probably at ~ 1 μb. With such limited results one must be careful not to draw too many conclusions. Fig. 9 shows both the energies of the first 2^+ state and the $B(\mathrm{E2}; 2^+ - 0^+)$ for these transitions plotted as a function of mass. The $B(\mathrm{E2})$ values are derived empirically from the energy of the 2^+ state according to the prescriptions of Grodzins [18] and Raman [19]. The $B(\mathrm{E2})$ values predicted by Möller and Nix [20] are also shown.

The results suggest that ^{76}Sr and ^{80}Zr are deformed in their ground states with $\beta \sim 0.35 - 0.4$. This is consistent with the prolate deformation expected in potential energy surface calculations [21]. This result was unexpected when first obtained since $N = Z = 40$ is a semi-magic number near stability. The result is confirmed by laser resonance fluorescence studies [22] of the properties of ^{77}Sr in its ground state. They show that $J^\pi = 5/2^+$, $\mu = 0.348\mu_n$ and $Q = +1.40(11)$b. This is consistent with the thirty-ninth and last neutron in ^{77}Sr being in the $[422]5/2^+$ orbital with $\beta_2 = +0.40$.

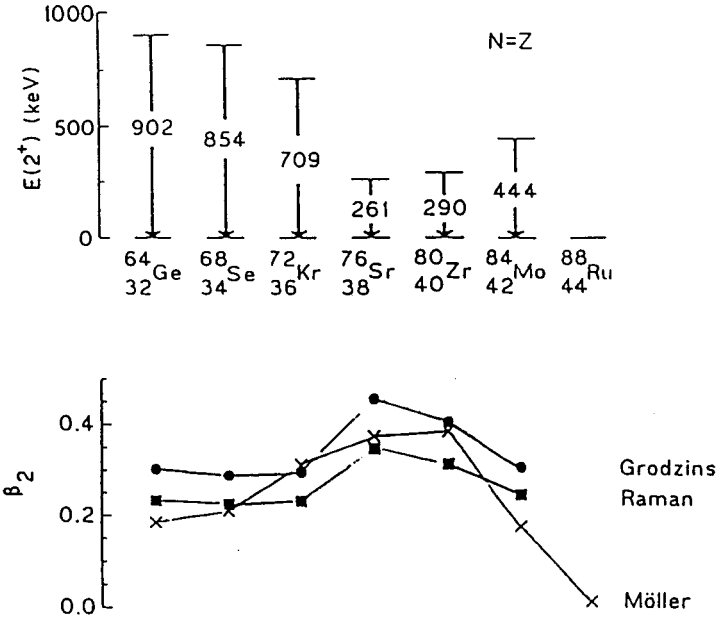

Fig. 9. The upper half shows the excitation energies of the first 2^+ states in the $N = Z$, even-even nuclei up to ^{84}Mo. The lower half shows the corresponding $(E2; 2^+ - 0^+)$ values derived from the $E(2^+)$ values (see text).

3. Future measurements

If one wishes to pursue any of the types of experiments described in Section 2.2. further how can we proceed? At least three ideas suggest themselves. Firstly one might use reaction channels involving α-particle emission such as the (α2n)-channel. So far in our experiments we were unable to detect γ-rays from these channels but perhaps one can find an efficient way of detecting them. Secondly one can use the brute force method, namely improve the efficiency of detection for both γ-rays and recoils. Thirdly one can use radioactive beams to produce more neutron-deficient compound nuclei which will enhance the channels leading to the $N = Z$ nuclei and may improve the experimental sensitivity.

3.1. Improved efficiency

It is possible to envisage a study of the ^{54}Fe (^{36}Ar,2n)^{88}Ru reaction at the ATLAS accelerator which would allow us to observe γ-rays in ^{88}Ru. The strategy adopted would be identical to that followed in the measurements at Daresbury. Now the recoils would be identified in an ionization chamber on

the end of the Fragment Mass Analyzer (FMA) [23] with the γ-rays being detected in ten EUROGAM style escape-suppressed Ge detectors.

If we assume that the 2n-reaction has a cross-section of 2μb, the intensity of the ^{36}Ar beam is 30pnA, the target thickness is 0.5mgcm^{-2} and that the FMA and γ-ray detection efficiencies are 15% and 2% respectively then one would estimate that two ^{88}Ru recoils should be detected per second. Hence in a five day run one would expect to see $\sim$ 2000 counts in the $2^+ - 0^+$ γ-ray peak, some twenty times more than was observed for ^{84}Mo.

It is proposed to carry out this experiment in the near future. To this end an ionization chamber has been built and installed behind the focal plane of the FMA. In tests with the ^{12}C(^{54}Fe,2n)^{68}Se reaction it showed the desired characteristics.

3.2. Radioactive beams

As stated earlier the use of radioactive nuclear beams (RNBs) with $N < Z$ on stable targets produces compound nuclei which are more neutron--deficient. As a result one may hope to populate the even-even, $N = Z$ nuclei more strongly than if stable beams are used. Whether this is so, depends on the intensities of the RNBs. The gain in cross-section may be offset by the likely loss in beam intensity. It has also been suggested that the radioactivity of the beam particles will increase the γ-ray background to the point where the sensitivity is again inadequate for the purpose.

At present a few different RNBs are available at Louvain-La-Neuve including ^{13}N and ^{19}Ne [24]. A small cyclotron producing 200 μA of 30 MeV protons is used to create ^{19}Ne in the ^{19}F(p,n)^{19}Ne reaction. The ^{19}Ne is ionised in an ECR source and then accelerated to the appropriate energy in a second cyclotron. Any residual ^{19}F is readily separated from the ^{19}Ne in the cyclotron. Beams of $10^8 - 10^9$p.p.s. of ^{19}Ne are available at 80 MeV.

To determine whether γ-rays from a fusion-evaporation reaction induced by a RNB can be studied we have studied [25] the γ-rays from the ^{40}Ca + ^{19}Ne reaction at a bombardment energy of 80 MeV with $\sim$ 150 ppA of ^{19}Ne. The target has a thickness of $\sim$ 1.6 mg cm^{-2}. The γ-rays were detected in eight escape suppressed Ge detectors of the TESSA type arranged in the backward hemisphere at 90° and 145°. Protons and alpha particles were detected in coincidence with the γ-rays in the LEDA Si-strip detector array [26]. The BGO shields were heavily protected by lead as was the beam dump situated 2m beyond the target. A piece of A1 foil of thickness 44 μ was placed in front of LEDA to stop the scattered beam particles reaching it.

Fig. 10 shows the γ-ray singles spectrum which appears to confirm one's worst fears since it is dominated by counts from the annihilation radiation. The second most prominent feature is gamma radiation from beta decay

which were produced in the ^{19}F induced reaction used to check the apparatus. The γ-rays of interest are only just visible.

Fortunately all is not lost. The cyclotron is pulsed and if one looks at the γ-ray spectrum during beam bursts, which is shown in Fig. 11 we see a very different picture. This spectrum was produced by adding counts to the spectrum during the beam on period and subtracting them when it was off. The annihilation radiation is eliminated and we see clearly γ-rays from the various open channels in the ^{40}Ca + ^{19}Ne reaction. It should be noted that one can observe the effects of finite lifetimes in the shapes of some of the lines.

The analysis of these data is at a very early stage. It is clear that the principal objective, to show that the γ-rays from fusion-evaporation reactions induced by RNBs can be studied, has been achieved. From the γ-γ coincidence data recorded during the experiment we can also build level schemes. We also expect to be able to extract cross-sections for the various reaction channels open at this beam energy for both the ^{19}F and ^{19}Ne beams. This comparison should allow us to determine whether there is an advantage in using the RNB to produce very neutron-deficient nuclei or not.

4. The production of radioactive nuclear beams

The case for building facilities to produce RNBs has been made in many places. It will not be repeated here. Suffice to say that one can envisage a wide range of uses of such beams in nuclear astrophysics, medicine, biology, condensed matter and atomic physics studies as well as in nuclear physics.

In addition if one envisages the burning of spent reactor fuel with intense beams of low energy protons one needs to know the relevant cross-sections as a function of energy. Since the isotopes of concern in the fuel rods are short-lived the only way we will be able to make such measurements is in inverse reactions on hydrogen with RNBs.

At high energies ($\geq$ 100 MeV/u) fragmentation is likely to remain the preferred method of RNB production. If intense beams near or below the Coulomb barrier are required the two accelerator method has the advantage. As in the example of the cyclotron complex described briefly above, one accelerator is needed to produce the radioactive species in an ion source/target system where the atoms of interest are ionised and then injected into a second accelerator to take the beam to the energy of interest.

Many reactions and beam species can be used to produce radioactive nuclei. There is a general consensus that the production method of choice is with intense beams of high energy protons. An excellent exemplar is the ISOLDE facility at CERN where beams of 2 μA of 1 GeV protons are used to generate radioactive species which are separated in mass and then

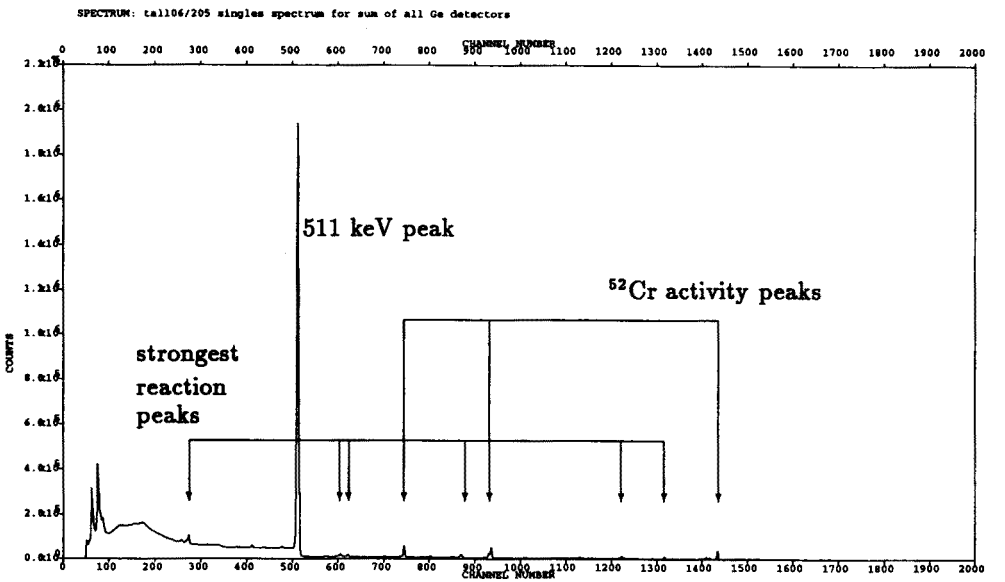

Fig. 10. Gamma ray singles spectrum recorded in the bombardment of ^{40}Ca with ^{19}Ne at Louvain-La-Neuve.

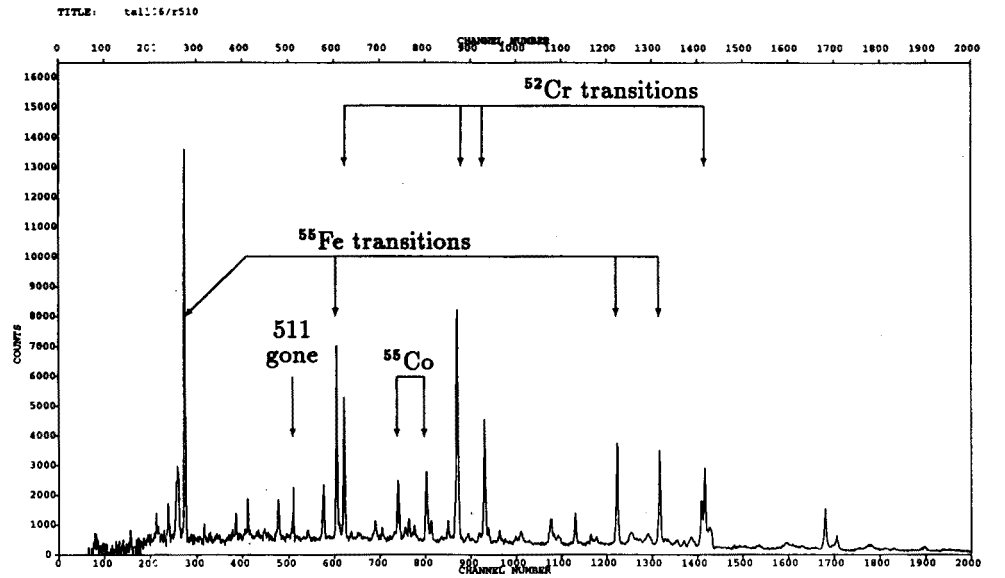

Fig. 11. The prompt γ-ray singles spectrum recorded from the ^{40}Ca + ^{19}Ne reaction studied at Louvain-La-Neuve.

accelerated to 60 keV energy. ISOLDE could provide the basis for a full scale RNB facility. The main limitation is the primary beam intensity since it is generally thought that 100 μA is needed for a full scale facility.

In the UK the pulsed neutron facility at the Rutherford Appleton Laboratory (RAL), ISIS [27], which currently has up to 200 μA of 800 MeV protons from a rapid cycling synchrotron, is well suited to provide the basis of an European intense RNB facility. The beam current in ISIS can be raised to $\sim$ 300 μA fairly readily. To add weight to the case ISIS also has an empty experimental hall which could house the Facility. The key to successful operation of such a facility is the ion source/target. The question to be answered before launching such a project is whether one can create ion sources and targets which will withstand 100 μA of beam and whether the yields of RNBs scale from 2 μA, where they are known, to 100 μA primary beam intensity.

Accordingly the Radioactive Ion Source Test (RIST) project has been set up at ISIS to answer the following questions:

a) Can one produce unstable nuclear species from a Ta target with 100 μA of 800 MeV protons?
b) Can one reproduce the yields from ISOLDE with 2 μA of beam from ISIS?
c) Do these yields scale with proton currents?
d) Can a stable voltage be maintained on the target platform under such bombardment?

The test facility and target design are shown schematically in Fig. 12. The target design is close to that of one type of ISOLDE target to facilitate comparison of the two. It consists of a stack of discs, each 25 μm thick and separated by 25 μm from its neighbour, welded to the inside of a tantalum tube. The tube is 25 cm in diameter and 20 cm long. It will absorb $\sim$ 30kW of proton beam power compared with 600 W at ISOLDE. The target will be heated to temperatures in the range 2000–2700 K to cause the short-lived species to diffuse rapidly out of target foils. At low currents the target will be heated by electron beam heating. After diffusion out of the target and into an ion source the atoms will be ionised on a hot tungsten surface. The cooling of the target will primarily be by thermal radiation to a secondary water cooled vacuum vessel.

As can be seen in Fig. 12 the RIST target will be inserted into the normal ISIS target position through a 4 m concrete plug in the ISIS shielding. The ISIS target will be retracted into a hutch where it will act as a beam dump. The ions will be extracted from the ion source across a 30 kV accelerating gap and into the optical system of the former Daresbury on-line separator which will be placed on top of the shielding superstructure. This will be used to separate the radioactive species by mass and transport them

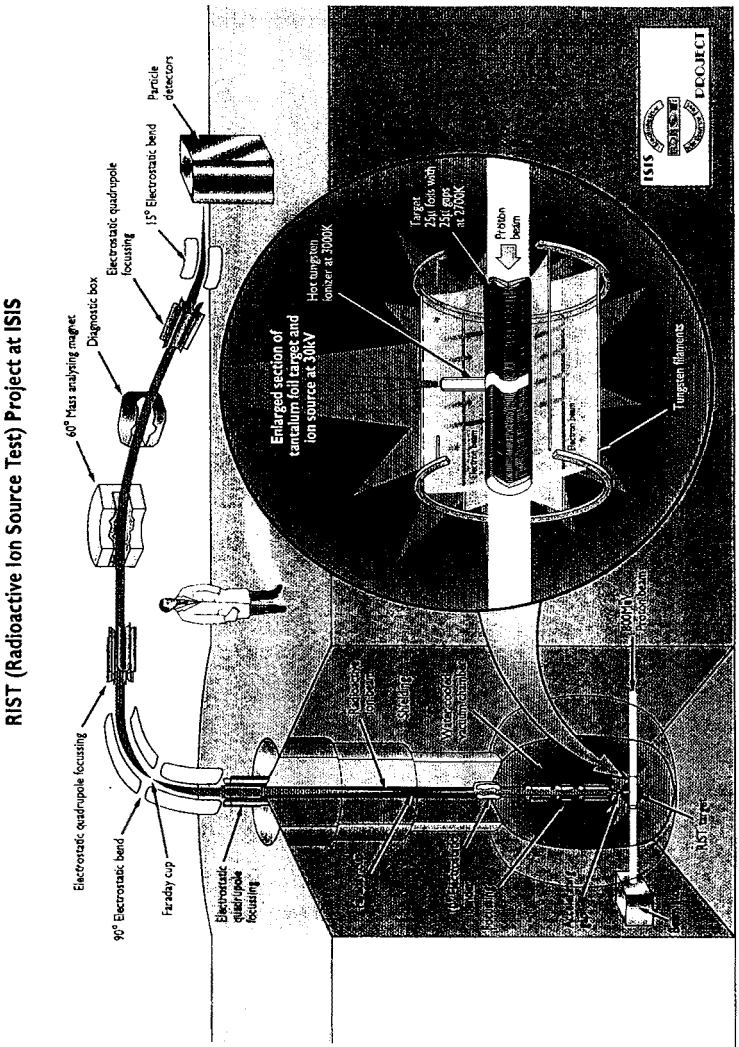

Fig. 12 A schematic diagram of the Radioactive Ion Source Test Facility at RAL.

to a target station where their yields can be measured.

This project is now well advanced with all of the materials available or on order. The first tests of the target assembly will be carried out at ISOLDE in December, 1994 to make a direct comparison of the RIST and ISOLDE targets under the same conditions. During 1995 the components of RIST will be assembled at ISIS and the test will be carried out in early 1996.

REFERENCES

[1] W. Nazarewicz *et al.*, *Nucl. Phys.* **A435**, 397 (1985).
[2] C. Baktash *et al.*, to be published.
[3] C.J. Lister *et al.*, *Phys. Rev.* **C42**, 1191 (1990).
[4] W. Gelletly *et al.*, *Phys. Lett.* **B253**, 287 (1991).
[5] J.A. Cameron *et al.*, *Phys. Lett.* **B235**, 239 (1990); J.A. Cameron *et al.*, *Phys. Rev.* **C44**, 1882 (1991).
[6] J.A. Cameron *et al.*, *Phys. Rev.* **C49**, 1347 (1994).
[7] R.K. Wallace, S.E. Woosley *Ap. J. Suppl.* **45**, 389 (1981).
[8] B.M. Sherrill, Proc. 2nd Int. Conf. on Radioactive Nuclear Beams, ed. T. Delbar, Adam Hilger, Bristol, Philadelphia and New York 1991, p.3.
[9] I. Tanihata *et al.*, *Phys. Rev. Lett.* **55**, 2676 (1985).
[10] R. Schneider *et al.*, *Z. Phys.* **A348**, 241 (1994).
[11] M. Lewitowicz *et al.*, *Phys. Lett.* **B332**, 20 (1994).
[12] B.M. Sherrill *et al.*, *Nucl. Instrum. Methods Phys. Res.* **B56/57**, 1106 (1991).
[13] M.F. Mohar *et al.*, *Phys. Rev. Lett.* **66**, 1571 (1991).
[14] J.A. Winger *et al.*, *Phys. Lett.* **B299**, 214 (1933).
[15] A.N. James *et al.*, *Nucl. Instrum. Methods Phys. Res.* **A267**, 144 (1988).
[16] P.J. Ennis *et al.*, *Nucl. Phys.* **A535**, 392 (1991).
[17] C.J. Gross *et al.*, to be published.
[18] L. Grodzins, *Phys. Lett.* **2**, 88 (1966).
[19] S. Raman *et al.*, *Phys. Rev.* **C43**, 556 (1991).
[20] P. Möller, J.R. Nix, *At. Data Nucl. Data Tables* **26**, 165 (1981).
[21] P. Möller, J.R. Nix, *At. Data Nucl. Data Tables* **39**, 225 (1988).
[22] P. Lievens *et al.*, *Phys. Rev.* **C46**, 797 (1992).
[23] C.N. Davids *et al.*, *Nucl. Instrum. Methods Phys. Res.* **B70**, 358 (1992).
[24] D. Darquennes *et al.*, *Phys. Rev.* **C42**, R804 (1990).
[25] W.N. Catford *et al.*, to be published.
[26] R. Coszach *et al.*, *Phys. Rev.* **C50**, 1695 (1994).
[27] J.L. Finney, *Europhys. News* **20**, (1989).